Received: 21 August 2020 | Revised: 1 September 2020 | Accepted: 1 September 2020

DOI: 10.1002/pol.20200590

ORIGINAL ARTICLE

JOURNAL OF POLYMER SCIENCE WILEY

Localized hydrogels based on cellulose nanofibers and wood pulp for rapid removal of methylene blue

Justin T. Harris | **Anne J. McNeil**

Department of Chemistry and Macromolecular Science and Engineering Program, University of Michigan, Ann Arbor, Michigan

Correspondence
Anne J. McNeil, Department of Chemistry and Macromolecular Science and Engineering Program, University of Michigan, Ann Arbor, MI 48109-1055.
Email: ajmcneil@umich.edu

Funding information
Directorate for Mathematical and Physical Sciences, Grant/Award Number: CHE-1740597

Abstract

Access to clean water has become increasingly difficult, motivating the need for materials that can efficiently remove pollutants. Hydrogels have been explored for remediation, but they often require long times to reach high levels of adsorption. To overcome this limitation, we developed a rapid, locally formed hydrogel that adsorbs dye during gelation. These hydrogels are derived from cellulose—a renewable, nontoxic, and biodegradable resource. More specifically, we found that sulfated cellulose nanofibers or sulfated wood pulps, when mixed with a water-soluble, cationic cellulose derivative, efficiently remove methylene blue (a cationic dye) within seconds. The maximum adsorption capacity was found to be 340 ± 40 mg methylene blue/g cellulose. As such, these localized hydrogels (and structural analogues) may be useful for remediating other pollutants.

KEYWORDS

cellulose nanofiber, cellulose wood pulp, chemical modification, dye adsorption, hydrogel

1 | INTRODUCTION

Accessible, clean water is increasingly scarce due to pollutants discharged in the environment.[1] Many localities across the United States are grappling with extensive groundwater contamination by persistent pollutants.[2] Organic dyes are one major source of pollution: 10–15% of the approximately 10^5 tons of dye produced globally each year have been released into the environment.[3] Moreover, dyes have been linked to a variety of health problems in humans and aquatic life.[3,4] To minimize the negative consequences of dye release, improved water remediation systems are needed.

Several strategies for removing dyes from the environment have been investigated, including chemical oxidation, membrane filtration, ion exchange, and most commonly, adsorption.[5–7] The primary adsorbent material employed for water purification is activated carbon because of its high capacity, porosity, and versatility in adsorbing different pollutants.[8] Despite these useful properties, making and regenerating activated carbon is costly and unsustainable,[8] leading researchers to explore alternative adsorbents.[6,9–12]

Cellulose, which can be sustainably sourced and is biodegradable, has been evaluated as an alternative adsorbent for water purification.[13–17] For example, Tam and coworkers reported that hydrogel beads made from sulfated cellulose nanocrystals (S-CNCs) and alginate could efficiently remove 97% of methylene blue (MB) from aqueous solutions.[18] In a different example, Yu and coworkers showed that carboxylated cellulose nanofiber (CNF) aerogels removed MB with up to 95% efficiency.[19] In both cases, however, the authors needed lengthy batch times (>30 min) to reach these high adsorption efficiencies, highlighting the need for alternative cellulose-based materials with a more rapid adsorption.

To overcome this challenge, we hypothesized that rapid adsorption might occur if dye adsorption and gel formation are simultaneous. The rationale is that the cellulosic binding sites are more accessible before and

during gelation, compared to after a gel has already formed. This approach was inspired by flocculating agents, which are commonly used in water treatment facilities.[20] Flocculants rapidly form a suspension when added to water, which allows for fast adsorption and easy removal through filtration. As a consequence, we hypothesized that an in situ-formed, localized (i.e., not sample-spanning), hydrogel could function like a flocculant, adsorbing pollutants while forming a suspended material for easy removal.

Both the hydrogel formation and adsorption processes need to be rapid for this approach to work. We anticipated that electrostatic crosslinking, which is both rapid and reversible, would be ideal for triggering localized gel formation (Scheme 1). We therefore targeted polyionic complexes,[21–24] which have previously been shown to form localized hydrogels in applications such as printable gels[25,26] and drug delivery systems.[27] In considering possible materials, we focused on cellulose-derived polymers due to their sustainable sourcing and biodegradability.

We initially focused on a system reported by Boluk and coworkers, wherein polyanionic S-CNCs and polycationic quaternized hydroxyethyl cellulose ethoxylate (QHECE) were mixed to form an all-cellulose based hydrogel.[28,29] Unfortunately, under their conditions, the gel formation was both slow (3 d) and not localized.[30] We hypothesized that longer cellulose fibers[31,32]—nanofibers (CNFs)[33–35] and wood pulp (WP)[36]—would create additional fiber/fiber entanglements, possibly enabling a faster-forming hydrogel.

Indeed, we report herein that sulfated CNFs (S-CNFs) and sulfated WPs (S-WPs) form localized hydrogels within 30 s when mixed with a water-soluble cationic cellulose derivative. In addition, we show that MB can be efficiently adsorbed while the localized gel forms, an advantage compared to traditional hydrogel adsorbents, which require lengthy batch times. Adsorption efficiencies above 90% are obtained across a wide range of dye concentrations, with a total adsorptive capacity of 340 mg dye/g cellulose. Both the solution pH and salt concentration had negligible effects on MB adsorption, indicating that the system is tolerant to a variety of water conditions. Overall, these locally formed cellulose-based hydrogels are effective adsorbents for cationic dyes and may be promising materials for other pollutants with alternative derivatization.

2 | EXPERIMENTAL

2.1 | Materials

Cellulose nanocrystals (spray-dried, Cellulose Lab Catalog Number CNC-SD) and cellulose nanofibrils (freeze-dried, Cellulose Lab Catalog Number CNF-FD) were purchased from Cellulose Lab. Bleached hardwood pulp was generously donated by Cellulose Lab. Chlorosulfonic acid and quaternized hydroxyethylcellulose ethoxylate (QHECE) were purchased from Aldrich and used without further purification. Deionized (DI) water purified by a Millipore Synergy water purification system was used as the water source, unless otherwise noted.

2.2 | Sulfation of CNF and WP

As described in detail below, the synthesis was performed similar to Kumar and coworkers.[37]

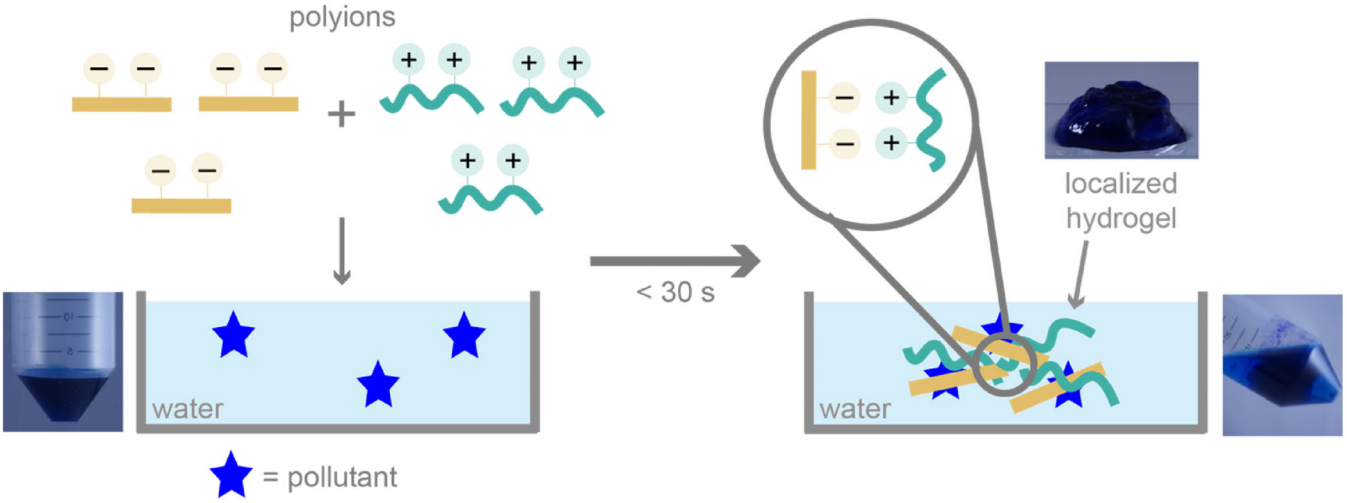

SCHEME 1 When combining oppositely charged polyions, a localized hydrogel forms via electrostatic crosslinks while rapidly adsorbing cationic pollutants [Color figure can be viewed at wileyonlinelibrary.com]

2.2.1 | CNF and WP dispersions

Unsulfated CNFs or WPs (400 mg) were placed in an oven-dried 100 ml flask with anhydrous DMF (50 mL), and the flask was capped with a septum. The mixture was soaked for 40 min without stirring under N_2. The mixture was then homogenized at a specified speed and time with an IKA T25 digital Ultra-Turrax (Table S1). The flask was recapped and soaked for 10 min under N_2. The mixture was homogenized a second time at a specified speed and time (Table S1). Then a stir bar was added, the flask was sealed, and the mixture was stirred for 40 min under N_2.

2.2.2 | CSA stock solution (2.0 M in DMF)

A Schlenk flask with stir bar and addition funnel were removed from the oven and assembled. The addition funnel was capped with a septum, and the system was cooled to room temperature under N_2. Anhydrous DMF (26 ml) was added to the Schlenk flask, and the solvent was cooled in an ice water bath for 10 min. Then, CSA (4 ml) was loaded into the addition funnel and added slowly over 5 min to the stirring DMF, with some HCl evolving. Once all the CSA was added, the addition funnel was removed and the Schlenk flask was capped, removed from the ice-water bath, and warmed to room temperature to provide a 2.0 M solution of CSA in DMF.

2.2.3 | CNF and WP sulfation

A specified amount of the 2.0 M CSA in DMF was added to the CNF or WP mixture dropwise over 0–2 min. The mixture was stirred for 20 min once all the CSA was added. Then, the reaction was quenched with methanol (~5 mL), and the mixture was stirred for 5 min.

The mixture was poured into a 250 mL centrifuge bottle, and the bottle was filled to ~90% capacity with DI water. The mixture was centrifuged at ~34,000 x g for ~25 min. The supernatant was discarded, and fresh DI water was added. Then a ~0.1 M NaOH solution was used to increase the pH to 7, as measured with pH paper. The mixture was centrifuged again at ~34,000*g* for ~25 min. The supernatant was discarded, and fresh DI water was added. The mixture was shaken by hand and then centrifuged a third time at ~34,000*g* for 25 min.

The fibers were then isolated using one of the two procedures described below. (a) If a white, gel-like mass remained in the centrifuge bottle, the supernatant was discarded, and the material was placed in smaller glass vials, frozen in liquid N_2, and dried under vacuum on a Schlenk line to remove excess water. (This procedure was used to access S-CNFs 0.77, 1.1, 1.5, 1.8, 1.9, and S-WP1.8.) (b) If the fibers did not form a gel-like mass in the centrifuge bottle, ~90% of supernatant was discarded, and the remaining mixture was vacuum filtered using a Whatman polyamide membrane filter (0.2 μm, 47 mm). The fibers on the filter were then rinsed once with DI water (5 mL), and placed in smaller glass vials, frozen in liquid N_2, and dried under vacuum on a Schlenk line to remove excess water. (This procedure was used to access S-WPs 0.53, 1.0, and 1.3.)

2.3 | Charge density measurements

Charge density measurements were carried out similar to the procedure given by Katz et al.[38,39] A known amount of S-CNFs or S-WPs (typically about 35 mg) was placed in a 20 ml vial with 0.1 M aq. HCl (15 ml) and a stir bar. The vial was capped and stirred for 90 min to protonate the S-CNFs or S-WPs. The mixture was then filtered over a polyamide membrane using vacuum filtration. The solids were rinsed with DI water until the conductivity of the filtrate was <10 μS/cm as measured by a Thermo Scientific Orion Star A215 pH/conductivity meter. The resulting solids were added to a tared 150 mL beaker followed by DI water (~20 ml) and a stir bar. The mixture was covered with weigh paper (of known mass), stirred for at least 5 min to uniformly disperse the solids, and then the stir bar was removed. The mixture was weighed to determine the total mass of the protonated S-CNF or S-WP mixture. Then, two aliquots of the mixture were removed, placed in separate tared 20 mL vials, accurately weighed (~2.5 g), and dried in a 110°C oven. For all samples (except S-CNF0.0 and S-WP0.0), the mass of solids in each aliquot was used to determine the concentration of solids in the protonated S-CNF or S-WP mixture. For S-CNF0.0 and S-WP0.0, the mass of solids in each aliquot overestimated the amount of fibers that were present (likely because the fibers were nonuniformly clumped together in the mixture), so the aliquot masses were subtracted from the initial amount of S-CNF0.0 or S-WP0.0 used to give a total amount of titrated S-CNF0.0 and S-WP0.0 fibers.

A stir bar and recorded volume (~100 mL) of 1 mM NaCl were then added to the beaker containing the protonated S-CNF or S-WP mixture. The mixture was titrated, with stirring, by adding a volume with known concentration of NaOH solution (~0.01 M) to the protonated S-CNF or S-WP mixture and measuring the conductivity of the mixture 40 s after each addition of titrant. (The concentration of the NaOH solution was

determined using the calibrated pH meter prior to the titration.) The volume-corrected conductivity was plotted as a function of the volume of NaOH added, and the equivalence point was determined by the intersection of the linear least-squares regression lines from the positively and negatively sloped regions of the curve (Figure S2). Based on the mmols of NaOH added, the mmol of SO_3^- were calculated. The charge density was found by dividing the mmol SO_3^- by the mass of S-CNF or S-WP that was titrated. This procedure was repeated and the average is reported as the sample's charge density (Table S2). Throughout the manuscript, S-CNF and S-WP samples will be identified by material type followed by the charge density (e.g., S-CNF1.1 is an S-CNF with a charge density of 1.1 mmol SO_3^-/g).

2.4 | Dye adsorption measurements

S-CNF1.8 (25.0 mg) was soaked in DI water (12.5 mL) for 5 min. The mixture was then homogenized at 10k rpm for 1 min to make a 0.200% w/v S-CNF1.8 mixture. QHECE (30.0 mg) was dissolved in DI water (20.0 mL) to make a 0.150% w/v QHECE solution. MB (60.0 mg, 188 μmol) was dissolved in DI water (6.0 mL) in a 50 mL centrifuge tube to make a 31 mM MB solution.

A volume of 31 mM MB solution was added to a 50 mL centrifuge tube followed by DI water to give a total volume of 2.0 mL. Then, 4.0 mL of 0.200% w/v S-CNF1.8 mixture and 4.0 mL of 0.150% w/v QHECE solution were added simultaneously, over a recorded time (Table S13), directly to the bottom of the centrifuge tube with vortex mixing at a speed setting of 1.5. The centrifuge tube was then vortex mixed using a speed setting of 1.5 for an additional recorded "mixing" time. The centrifuge tube was then removed from the vortex mixer, and a gel was observed. An aliquot of water was removed from the centrifuge tube, placed in a cuvette, and the absorbance spectrum of the solution from 400 to 750 nm was obtained. The UV–vis measurement was performed within 1 min of the gel being formed. The absorbance spectrum for each gel sample was obtained and baseline corrected (Supporting Information, p. S38). The corrected absorbance at 661 nm was then recorded for each gel sample, and the concentration of MB that was not adsorbed was determined using a calibration curve (Figure S34).

2.5 | Dye desorption study

0.200% w/v S-CNF1.8 mixtures, 0.150% w/v QHECE solutions, and a 31 mM MB solution were prepared according to the procedure in the "Dye adsorption measurements" section. An "acidic ethanol" solution (1:1 (v:v) EtOH:0.10 M aq. HCl solution, 50.0 ml) was prepared in a 50 ml polypropylene centrifuge tube ("Tube 1"). The tube was wrapped in aluminum foil to minimize light, and set aside for later use.

DI water (1.92 mL) was combined with an aliquot of 31 mM MB solution (80.0 μl) in a 50 ml polypropylene centrifuge tube ("Tube 2"), and the solution was vortex mixed using a speed setting of 1.5 for 15 s. Then, S-CNF1.8-based gels were produced according to the procedure in the "Dye adsorption measurements" section. After a gel was formed, the gel was removed from Tube 2 using a spatula and placed into Tube 1. Tube 1 was capped and placed in a closed, dark drawer. Then, an aliquot of leftover solution from Tube 2 was placed in a cuvette, and an absorbance spectrum from 400 to 750 nm was obtained and baseline corrected. The corrected absorbance at 661 nm was then recorded for each gel sample, and the mass of adsorbed MB (MAMB) that was adsorbed was determined using a calibration curve.

Then, at recorded time intervals, Tube 1 was removed from the drawer and inverted to mix the contents of the tube. An aliquot of solution was then placed in a cuvette, and the absorbance spectrum of the solution was obtained and corrected. The aliquot was returned to Tube 1, and the tube was placed back in a closed drawer. For the aliquots removed from Tube 1, the mass of desorbed MB (MDMB) in solution at each time point was determined using a separate calibration curve that was generated for MB in acidic ethanol (Figure S45). The MB desorption % was then calculated at each time point using the following equation:

$$\text{MB desorption}\% = \frac{\text{MDMB}}{\text{MAMB}} \times 100 \quad (1)$$

This procedure was performed for three hydrogel samples (Table S25 and Figure S47), and an average MB desorption % after 24 hr is reported based on these samples.

3 | RESULTS AND DISCUSSION

3.1 | Identifying conditions for quick-forming, localized hydrogels

As described above, we hypothesized that cellulose materials with longer lengths would generate more (physical) crosslinking sites, which would potentially lead to a faster, localized gelation. We also hypothesized that higher charge densities would lead to faster gelation due to rapid charge/charge interactions generating more

(physical) crosslinks. To test both these hypotheses, we functionalized CNFs and WPs by reacting them with varying amounts of chlorosulfonic acid.[40,41] Previous studies on cellulose functionalization suggest that the sulfation likely occurs at the C6 and C2 positions on the glucose repeat unit.[42] Materials with charge densities ranging from 0.0 to 1.9 mmol SO_3^-/g were generated, as determined by conductometric titrations. Elemental analyses performed on a subset of samples showed that the conductometric titrations are accurate (i.e., less than 0.25% difference in S content, Table S3). The charge density on the other hydrogel component (commercial QHECE) was measured herein to be 1.23 mmol R_4N^+/g (Supporting Information, pp. S7–S8). SEM images indicate that the size of S-CNFs and S-WPs did not change significantly after functionalization, but small changes in S-CNF structure (e.g., some fracturing) were observed for some charge densities (Supporting Information, pp. S9–S12).

Localized gels[43] were formed within seconds when QHECE solutions were added to suspensions of aq. S-CNF or S-WP (Figure 1 and Supporting Information, pp. S13–S18). Gel formation was impacted, as anticipated, by the CNF and WP charge density as well as by the molar charge ratio (f^-), which is the ratio of negative charges to total charge. For example, S-CNF-based gels only formed with a charge density ≥0.77 mmol SO_3^-/g and an $f^- \geq 0.39$. Similarly, S-WP-based gels only formed with a charge density ≥ 0.53 mmol SO_3^-/g and an $f^- \geq 0.30$. Both results indicate that there is a minimum amount of negative charge necessary to interact with QHECE and form an electrostatically crosslinked gel.

In both cases, gel formation was rapid (within 30 s) and localized, possibly driven by the entropy gain from the release of counterions into solution.[44] Surprisingly, the shorter S-CNFs formed gels at lower concentrations than the longer S-WPs, even when the charge densities were similar. (Localized gels could be formed with as little as 0.010% S-CNF and 0.0050% w/v QHECE.) This result is likely due to the thinner CNFs having more fiber/fiber interactions and entanglements compared to the same mass of the thicker WP. The S-CNF-based gels also exhibited higher swelling ratios relative to the analogous S-WP-based gels under otherwise identical conditions (Supporting Information, pp. S19–S27). This result may be attributable to the larger interstitial volume present in gels made from the thinner S-CNF fibers, leading to more water retention via capillary forces.[45]

Examining the mass balance revealed that approximately 40–60% of the added cellulose was incorporated into the gels (Supporting Information Tables S9 and S11). Most likely, the water-soluble QHECE is the dominant species in solution. The mechanical properties of the isolated S-CNF and S-WP hydrogels were probed using oscillatory shear rheology (Supporting Information, pp. S28–S32). The elastic modulus (G') was nearly independent of frequency and greater than storage modulus (G'') in the frequency range of 0.1–50 rad/s. These results are characteristic of physical hydrogels.

Overall, the rapid, localized gel formation observed with both S-CNFs and S-WPs, suggests that the longer fiber lengths and higher charge densities played an important role, presumably by creating additional crosslinks. For the rest of the studies, we focused on the hydrogels made from S-CNFs with the highest charge density (1.8 mmol SO_3^-/g) because we anticipated that the highest adsorption would be achieved with gels containing the most negative sites.

3.2 | Assessing dye adsorption

Because the insoluble cellulose component was anionic, we anticipated that these hydrogels would be best at adsorbing dyes with cationic charge. Gratifyingly, we observed over 90% MB adsorption within 1 min when the dye concentration was <400 μM (Figure 2 and Figure 3a, Supporting Information Video #3). This

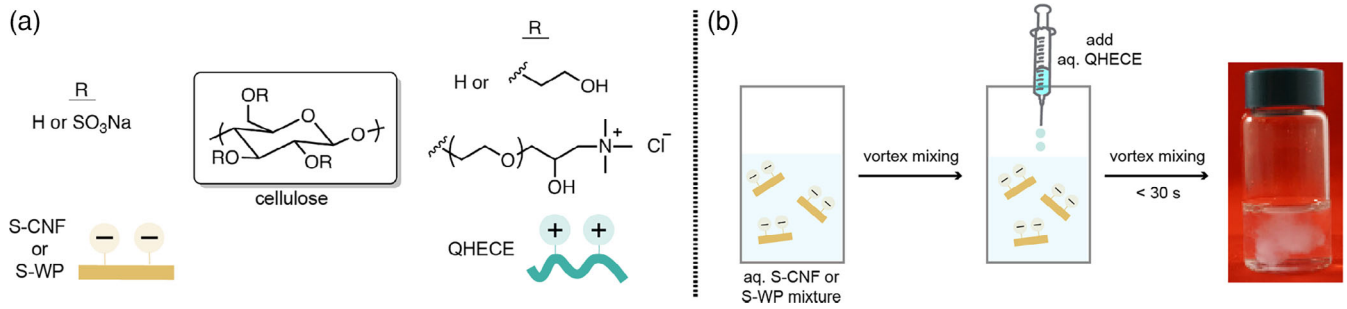

FIGURE 1 (a) Chemical structures for S-CNFs, S-WPs, and QHECE. (b) Procedure for making hydrogels (see also, Supporting Information Video #2). The gel shown is made from 0.050% w/v S-CNF1.9 and QHECE [Color figure can be viewed at wileyonlinelibrary.com]

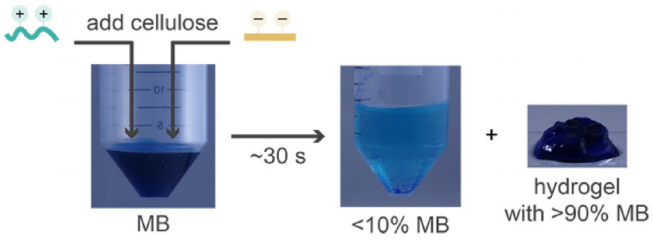

FIGURE 2 A localized hydrogel formed after adding aq. QHECE and S-CNF mixtures to an aq. solution containing MB ($[MB]_i$ = 94 μM; $[S\text{-}CNF1.8]_f$ = 0.08% w/v; $[QHECE]_f$ = 0.06% w/v) [Color figure can be viewed at wileyonlinelibrary.com]

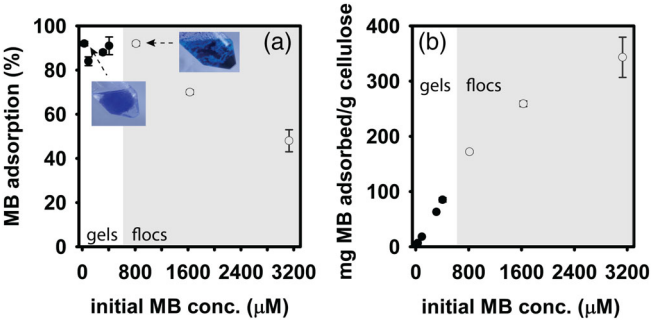

FIGURE 3 (a) MB adsorption percent as a function of the initial dye concentration for S-CNF1.8 gels (●) and flocs (○). (b) MB adsorption capacity as a function of the initial dye concentration for S-CNF1.8 gels (●) and flocs (○). All gels and flocs were made using 0.080% w/v S-CNF1.8 and 0.060% w/v QHECE [Color figure can be viewed at wileyonlinelibrary.com]

adsorption % held true as long as the ratio of dye/negative sites was kept below 0.35. MB adsorption only slightly increased over time (e.g., 96% at 3 min to 99% at 3000 min), likely due to a slower process of MB diffusion into the internal sites within the CNF fibers (Table S17).[46,47] The maximum capacity for MB adsorption was 94.5 ± 0.2 mg dye/g cellulose under these conditions.

At higher MB concentrations, we observed something similar to flocculation; rather than a single, localized hydrogel forming, we observed several smaller flocs.[48] Under these conditions, there is more MB than negative sites, leading to lower adsorption, and weaker gels. The maximum capacity for MB adsorption under these conditions was 340 ± 40 mg dye/g cellulose (Figure 3b). This value slightly outperforms related materials from the literature, with 256 mg dye/g of cellulose for CNC-based hydrogel beads reported by Tam and coworkers,[18] and 128 mg MB/g of cellulose for CNF-based aerogels reported by Yu and coworkers.[19] The advantage of our system (over these examples) is the rapid speed for both the adsorption (<5 min) and gelation processes (<30 s).

We hypothesized that the MB/gel interactions were largely driven by charge complexation. To test this hypothesis, we first evaluated MB adsorption to S-CNF alone. Under conditions similar to above, the S-CNFs adsorbed approximately 85% of the MB, consistent with a charge-based complexation (Table S26). In a separate experiment, when an S-CNF with a lower charge density was used to form a gel, and all other variables were held constant, the maximum adsorption decreased (160 ± 30 mg dye/g cellulose, Table S20). This result also suggests that the primary driving force for adsorption is charge complexation. In addition, this result suggests that higher adsorption capacities might be accessible with higher S-CNF charge densities.

To demonstrate the advantages of having adsorption occur simultaneously with gelation, we added a preformed hydrogel into a solution of MB and monitored its adsorption over time. Gratifyingly, we observed slow adsorption with the preformed gel (e.g., 20% at 2 min) compared to in the in situ system (>90% at 2 min). Only after 60 min did the preformed gel reach the same adsorption levels as our simultaneous system.

3.3 | Effect of salt concentration and pH on dye adsorption

Industrial effluent from dye manufacturing contains many other dissolved species, including acids and bases.[19] As such, we examined the influence of both salt concentration and solution pH on dye adsorption.

No significant decrease in dye adsorption was observed over a pH range of 2.5–11.5 (Figure 4a). These results were expected because there should be no change in charge for any of the species over this pH range. More specifically, QHECE is a quaternized amine with four alkyl groups, giving it a pH-insensitive permanent charge. The sulfate on the S-CNFs have an estimated pKa ~ 2,[49] indicating that they will be fully deprotonated under our conditions. Similarly, MB has an estimated pKa ~ 3[50] and is expected to be cationic over the pH range examined.

We also found that as salt concentration increases (from 0), the MB adsorption remains constant (Figure 4b), suggesting that Na^+ is not displacing the MB under these conditions.[51] However, gelation was inhibited above ~99 mM NaCl, indicating that the electrostatic-based crosslinking between S-CNF and QHECE was being disrupted.

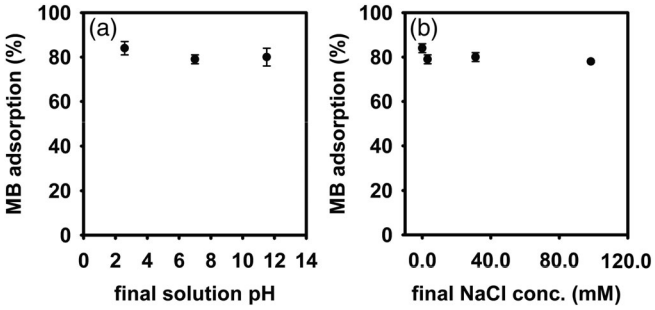

FIGURE 4 MB adsorption as a function of (a) pH and (b) NaCl concentration for S-CNF/QHECE hydrogels ([MB] = 94 μM, [S-CNF1.8] = 0.080% (w/v); [QHECE] = 0.060% (w/v))

3.4 | Dye desorption

For water treatment applications, it would be advantageous to desorb the MB dye so that the cellulose-based gel can be reused or biodegraded. As such, we soaked the used hydrogels in acidic EtOH (pH = 1.55) for 24 hr (Supporting Information, pp. S56–S59).[18,52] Subsequent UV–vis spectroscopic analysis of the supernatant revealed approximately 55 ± 2% of the MB had desorbed, presumably via competitive binding of the H^+ to the sulfate groups. Clearly, further optimization will be necessary to fully recycle or recapture the spent materials.

4 | CONCLUSIONS

In summary, functionalized cellulose nanofibers and wood pulp were found to form localized hydrogels with an oppositely charged, water-soluble cellulose derivative, driven by electrostatic and physical crosslinking. These localized gels rapidly adsorb cationic dye during gelation, giving them an advantage over traditional hydrogel-based adsorbents. The maximum adsorption capacity was found to be 340 ± 40 mg methylene blue/g cellulose, which outperformed other cellulose-based physical gels.

Overall, we anticipate that these and related localized hydrogels may have future applications as flocculating agents in water purification. Moving forward, we intend to tailor the localized hydrogels to adsorb other contaminants that threaten freshwater supplies.[2,16,53] Toward this goal, we have successfully removed anionic dyes with cationic wood pulp-based gels. These and related studies will be reported in due course.

ACKNOWLEDGMENTS

We gratefully acknowledge the National Science Foundation for supporting this work through a Phase I Center for Chemical Innovation Grant (CHE-1740597). We thank Joelle Anderson for assistance with taking the photos and videos of gel formation, Cellulose Lab for generously providing wood pulp, and the Robert B. Mitchell Electron Microbeam Analysis Lab for use of their imaging facilities, and Dr. Owen Neill for SEM training and expertise.

CONFLICT OF INTEREST

The authors declare no competing financial interests.

ORCID

Justin T. Harris https://orcid.org/0000-0002-6495-8248
Anne J. McNeil https://orcid.org/0000-0003-4591-3308

REFERENCES AND NOTES

[1] A. Boretti, L. Rosa, *npj Clean Water* **2019**, *2*. https://www.nature.com/articles/s41545-019-0039-9
[2] U.S.E.P.A., https://ofmpub.epa.gov/waters10/attains_nation_cy.control (accessed: April 24, 2020).
[3] K. A. Wani, N. K. Jangid, A. R. Bhat Eds., *Impact of Textile Dyes on Public Health and the Environment*, IGI Global, Pennsylvania **2020**.
[4] S. Khan, A. Malik, in *Environmental Deterioration and Human Health* (Eds: A. Malik, E. Grohmann, R. Akhtar), Springer, Dordrecht **2014**, p. 55.
[5] M. A. M. Salleh, D. K. Mahmoud, W. A. W. A. Karim, A. Idris, *Desalination* **2011**, *280*, 1.
[6] N. B. Singh, G. Nagpal, S. Agrawal, Rachna, *Environ. Technol. Innov.* **2018**, *11*, 187.
[7] M. T. Yagub, T. K. Sen, S. Afroze, H. M. Ang, *Adv. Colloid Interface Sci.* **2014**, *209*, 172.
[8] S. J. T. Pollard, G. D. Fowler, C. J. Sollars, R. Perry, *Sci. Total Environ.* **1992**, *116*, 31.
[9] A. H. Shalla, M. A. Bhat, Z. J. Yaseen, *Environ. Chem. Eng.* **2018**, *6*, 5938.
[10] V. Van Tran, D. Park, Y. C. Lee, *Environ. Sci. Pollut. Res.* **2018**, *25*, 24569.
[11] H. Wang, X. Ji, M. Ahmed, F. Huang, J. L. Sessler, *J. Mater. Chem. A* **2019**, *7*, 1394.
[12] M. S. de Luna, R. Altobelli, L. Gioiella, R. Castaldo, G. Scherillo, G. Filippone, J. Polym, *Sci., Part B: Polym. Phys.* **2017**, *55*, 1843.
[13] C. Chang, L. Zhang, *Carbohydr. Polym.* **2011**, *84*, 40.
[14] S. Hokkanen, A. Bhatnagar, M. Sillanpää, *Water Res.* **2016**, *91*, 156.
[15] H. Kang, R. Liu, Y. Huang, *Macromol. Chem. Phys.* **2016**, *217*, 1322.
[16] N. Mohammed, N. Grishkewich, K. C. Tam, *Environ. Sci. Nano* **2018**, *5*, 623.
[17] A. G. Varghese, S. A. Paul, M. S. Latha, *Environ. Chem. Lett.* **2019**, *17*, 867.
[18] N. Mohammed, N. Grishkewich, R. M. Berry, K. C. Tam, *Cellulose* **2015**, *22*, 3725.
[19] D. Wang, H. Yu, X. Fan, J. Gu, S. Ye, J. Yao, Q. Ni, *ACS Appl. Mater. Interfaces* **2018**, *10*, 20755.
[20] E. M. Wilts, J. Herzberger, T. E. Long, *Polym. Int.* **2018**, *67*, 799.

[21] J. Berger, M. Reist, J. M. Mayer, O. Felt, R. Gurny, *Eur. J. Pharm. Biopharm.* **2004**, *57*, 35.
[22] S. D. Hujaya, G. S. Lorite, S. J. Vainio, H. Liimatainen, *Acta Biomater.* **2018**, *75*, 346.
[23] V. S. Meka, M. K. G. Sing, M. R. Pichika, S. R. Nali, V. R. M. Kolapalli, P. Kesharwani, *Drug Discovery Today* **2017**, *22*, 1697.
[24] T. Ingverud, E. Larsson, G. Hemmer, R. Rojas, M. Malkoch, A. Carlmark, *J. Polym. Sci., Part A: Polym. Chem.* **2016**, *54*, 3415.
[25] H. Cui, Y. Yu, X. Li, Z. Sun, J. Ruan, Z. Wu, J. Qian, J. Yin, *J. Mater. Chem. B* **2019**, *7*, 7207.
[26] W. L. Ng, W. Y. Yeong, M. W. Naing, *Int. J. Bioprint.* **2016**, *2*, 53.
[27] Y. Tang, C. L. Heaysman, S. Willis, A. L. Lewis, *Expert Opin. Drug Deliv.* **2011**, *8*, 1141.
[28] A. Lu, Y. Song, Y. Boluk, *Carbohydr. Polym.* **2014**, *114*, 57.
[29] A. Lu, Y. Wang, Y. Boluk, *Carbohydr. Polym.* **2014**, *105*, 214.
[30] We were able to obtain faster-forming hydrogels (350 s) with higher concentrations of both S-CNCs and QHECE (2.0% w/v each). With further optimization, hydrogels could be formed in 75 s with as little as 1.0% (w/v) S-CNCs and 0.5% (w/v) QHECE (Supporting Information Video #1 and Figure S1).
[31] K. J. De France, T. Hoare, E. D. Cranston, *Chem. Mater.* **2017**, *29*, 4609.
[32] M. S. Reid, M. Villalobos, E. D. Cranston, *Langmuir* **2017**, *33*, 1583.
[33] D. Klemm, F. Kramer, S. Moritz, T. Lindström, M. Ankerfors, D. Gray, A. Dorris, *Angew. Chem. Int. Ed.* **2011**, *50*, 5438.
[34] D. Klemm, E. D. Cranston, D. Fischer, M. Gama, S. A. Kedzior, D. Kralisch, F. Kramer, T. Kondo, T. Lindström, S. Nietzsche, K. Petzold-Welcke, F. Rauchfuß, *Mater. Today* **2018**, *21*, 720.
[35] F. H. A. Rodrigues, C. Spagnol, A. G. B. Pereira, A. F. Martins, A. R. Fajardo, A. F. Rubira, E. C. Muniz, *J. Appl. Polym. Sci.* **2014**, *131*, 1.
[36] S. Sousa, A. P. Costa, R. Simões, *Composites, Part A* **2019**, *121*, 273.
[37] J. Luo, N. Semenikhin, H. Chang, R. J. Moon, S. Kumar, *Carbohydr. Polym.* **2018**, *181*, 247.
[38] S. Katz, R. P. Beatson, A. M. Scallan, *Sven. Papperstidn.* **1984**, *87*, R48.
[39] S. Pan, A. J. Ragauskas, *Carbohydr. Polym.* **2014**, *111*, 514.
[40] Y. Wang, X. Wang, Y. Xie, K. Zhang, *Cellulose* **2018**, *25*, 3703.
[41] L. Zhu, J. Qin, X. Yin, L. Ji, Q. Lin, Z. Qin, *Polym. Adv. Technol.* **2014**, *25*, 168.
[42] S. Eyley, W. Thielemans, *Nanoscale* **2014**, *6*, 7764.
[43] M. Costalat, P. Alcouffe, L. David, T. Delair, *Carbohydr. Polym.* **2015**, *134*, 541.
[44] J. Fu, J. B. Schlenoff, *J. Am. Chem. Soc.* **2016**, *138*, 980.
[45] Y. Zhou, S. Fu, L. Zhang, H. Zhan, *Carbohydr. Polym.* **2013**, *97*, 429.
[46] F. Jiang, D. M. Dinh, Y. Lo Hsieh, *Carbohydr. Polym.* **2017**, *173*, 286.
[47] H. Deng, J. Lu, G. Li, G. Zhang, X. Wang, *Chem. Eng. J.* **2011**, *172*, 326.
[48] Rheological studies performed on these flocs were consistent with a weak, physical gel; however, this result may be an artifact due to the compression of the flocs during sample preparation (Supporting Information, pp. S32–S37).
[49] H. Wang, C. Qian, M. Roman, *Biomacromolecules* **2011**, *12*, 3708.
[50] A. R. Disanto, J. G. Wagner, *J. Pharm. Sci.* **1972**, *61*, 1086.
[51] N. S. Maurya, A. K. Mittal, P. Cornel, E. Rother, *Bioresour. Technol.* **2006**, *97*, 512.
[52] J. Hua, R. Meng, T. Wang, H. Gao, Z. Luo, Y. Jin, L. Liu, J. Yao, *Fibers Polym.* **2019**, *20*, 794.
[53] L. Xiao, C. Ching, Y. Ling, M. Nasiri, M. J. Klemes, T. M. Reineke, D. E. Helbling, W. R. Dichtel, *Macromolecules* **2019**, *52*, 3747.

SUPPORTING INFORMATION

Additional supporting information may be found online in the Supporting Information section at the end of this article.

How to cite this article: Harris JT, McNeil AJ. Localized hydrogels based on cellulose nanofibers and wood pulp for rapid removal of methylene blue. *J Polym Sci*. 2020;58:3042–3049. https://doi.org/10.1002/pol.20200590